Advance View
https://doi.org/10.3354/meps14331

MARINE ECOLOGY PROGRESS SERIES
Mar Ecol Prog Ser

August 3, 2023

Contribution to the Theme Section 'Species range shifts, biological invasions and ocean warming'

Influence of extreme cold and warm oceanographic events on larval fish assemblages in the southern region of the California Current

Gerardo Aceves-Medina[1,*], Ana Gabriela Uribe-Prado[1], Sylvia Patricia Adelheid Jiménez-Rosenberg[1], Reginaldo Durazo[2], Ricardo J. Saldierna-Martínez[1], Raymundo Avendaño-Ibarra[1], Airam Nauzet Sarmiento-Lezcano[3]

[1]Instituto Politécnico Nacional, Centro Interdisciplinario de Ciencias Marinas, Apartado Postal 592, 23096 La Paz, BCS, México
[2]Facultad de Ciencias Marinas, Universidad Autónoma Baja California, 22860, Ensenada, BC, México
[3]Instituto de Oceanografía y Cambio Global, IOCAG, Universidad de Las Palmas de Gran Canaria, Campus de Taliarte, 35214 Telde, Gran Canaria, Canary Islands, Spain

ABSTRACT: The larval fish community in the southern region of the California Current (CC) was analyzed to test the hypothesis of a northward expansion of tropical species for the summer–fall seasons of La Niña (LN) 2010–2011, The Blob 2014, and El Niño (EN) 2015–2016. Interannual temperature anomalies (–5 to +2°C), as well as decreases in chlorophyll *a* (68%) and zooplankton density (71%), resulted in dramatic changes in the larval fish community, such as an 82% decline in larval fish density, unprecedented for the CC. Tropical species richness increased in the north by 46%, while temperate species decreased by 65% in the south. Mesopelagic species richness and relative abundance increased in the north by 53 and 92%, respectively. In the south, the species richness of the demersal component increased up to 39%, although demersal species were co-dominant with mesopelagic species, accounting for 47% of the relative abundance compared to 49% for the mesopelagic species. The magnitude of the changes in the community was unparalleled when compared with other warming events, such as EN 1983–1984 or EN 1997–1998. The differences were probably related to the presence of The Blob, which favored the transport of oceanic species into the neritic region of the CC. In both cold and warm years, fronts and mesoscale eddies in the middle part of the Baja California Peninsula represented barriers to the latitudinal distribution of species, even during intense tropicalization processes, since no latitudinal extensions in species distribution occurred.

KEY WORDS: Fish larvae · Southern California Current Region · La Niña 2010–2011 · El Niño 2015–2016 · The Blob 2014 · Marine heatwave

1. INTRODUCTION

Three major climatic events influenced the dynamics of the California Current System (CCS) from 2010 to 2016. In the late spring of 2010, the CCS experienced a strong La Niña (LN) event, characterized by cool ocean conditions followed by strong upwelling (Rudnick et al. 2017). After the spring of 2012, the CCS returned to mean climatological values (Bjorkstedt et al. 2012), but from 2013 to 2016, several pronounced changes to the physical and biological oceanographic dynamics of the Northeast Pacific led to strong ocean warming. First, there was the warming of the surface waters of the Northeast-

*Corresponding author: gaceves@ipn.mx

ern Pacific by a marine heatwave (MHW) known as 'The Blob'. The Blob started in 2013 off the coast of Alaska, and by the spring of 2014, it had reached the northern west coast of the Baja California Peninsula (WBCP) in Mexico and persisted until 2015 (Peterson et al. 2017). This was followed by one of the three most intense recorded El Niño (EN) events, which peaked in the winter of 2015–2016 (Fiedler & Mantua 2017).

The combination of the 2013–2016 ocean warming events created an unprecedented warm period in which the mean annual sea surface temperature (SST) for 2015 was the highest since 1920 (1.7°C SST anomaly) when the records began, and the mean SST from 2014 to 2016 was the highest over any other consecutive 3 yr period (1.3°C anomaly; Jacox et al. 2018). This warm period had a strong impact on species distributions along the US west coast, especially in adult and larval fishes (Auth et al. 2015, 2018, Walker et al. 2020, Nielsen et al. 2021, Thompson et al. 2022). However, up until the present it was unknown how this sequence of events affected the pelagic ecosystems in the southern region of the CCS.

The WBCP is the southern limit of the CCS and is dominated by several currents: the equatorward California Current (CC), which is an extension of the North Pacific anticyclonic gyre; the California Undercurrent (CU) with a subsurface poleward flow between 100 and 400 m that originates in the Eastern Equatorial Pacific; and the California Countercurrent (CCC) that discontinuously transports warm water toward the pole over the continental slope (Durazo et al. 2010). These currents change in intensity due to wind seasonality. During the spring and summer upwelling season, the alongshore, northwesterly winds are more intense, strengthening the CC (Durazo 2015). In fall and winter, winds from the southeast predominate, weakening the CC, intensifying the CCC, and reducing upwelling (Valle-Rodríguez & Trasviña-Castro 2017).

Several studies carried out on the WBCP have observed a faunistic transition zone off Punta Eugenia (PE), characterized by the presence of a complex of temperate-affinity species to the north and species of tropical–subtropical affinity to the south (Moser & Smith 1993, Jiménez-Rosenberg et al. 2010). The boundary between faunistic northern and southern species complexes is theoretically displaced northward during EN events and southward during LN (Aceves-Medina et al. 2018). Effects of tropicalization due to EN in the southern region of the CCS are not always the same. Although there is strong evidence of tropicalization from southern California to Oregon, USA, during the 2013–2016 warming events (McClatchie et al. 2018), there is no information on how these events affected the epipelagic marine ecosystem off the Baja California Peninsula, particularly the larval fish community. This study aimed to examine the impact that the transition between the strong LN 2010–2011 to the unprecedented warm period of 2014–2016 had on the distribution and abundance of the larval fish assemblages during summer–fall periods.

2. MATERIALS AND METHODS

2.1. Sample collection

The environmental data and zooplankton samples came from 3 oceanographic surveys carried out on RVs 'Francisco de Ulloa' and 'BIPO-INAPESCA'. The 2011 fall survey (IMECOCAL-1110; 4–21 October 2011) consisted of 75 sampling stations between Ensenada, Baja California (BC), and the Gulf of Ulloa, Baja California Sur (BCS), while both summer of 2014 (BIPOCO-1407; 14 July to 13 September 2014) and summer–fall of 2015 (BIPOCO-1509; 17 September to 30 October 2015) surveys included 188 sampling stations each, between Ensenada, BC, and Cabo San Lucas, BCS (Fig. 1). In all cases, stations were sampled at 20 n mile intervals along transects perpendicular to the coast, which were separated by 40.5 n miles.

At each station, the pressure, conductivity, temperature, and fluorescence in the water column were measured to a maximum depth of 1500 m using a CTD (Seabird SBE-911plus in 2011 and 2014, and Idronaut Ocean Seven 320 plus in 2015). CTD data were used to derive salinity (psu), chlorophyll *a* con centration (chl *a*; mg m^{-3}), and mixed layer depth (MLD; m) for each station. In addition, satellite mean sea level anomalies (MSLAs; cm) and their associated geostrophic flows were obtained from the Copernicus Marine Environment Monitoring Service (CMEMS, http://marine.copernicus.eu) and were used to portray the regional circulation patterns during each survey. The water masses were determined with temperature-salinity (T-S) diagrams according to the ranges proposed by Durazo & Baumgartner (2002).

Zooplankton samples were collected with oblique trawls of cylindrical-conical Bongo nets, at a maximum depth of 210 m (Smith & Richardson 1977). The mouth diameter of the nets was 0.71 m, with a mesh opening of 505 µm. Nets were equipped with a digital flow meter (General Oceanics) to estimate the vol-

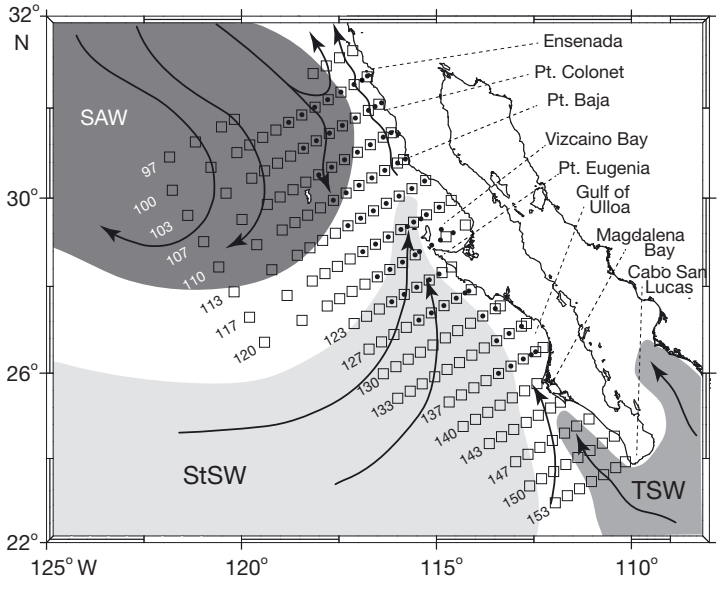

Fig. 1. Study area and sampling stations during fall 2011 (•), summer 2014, and summer–fall 2015 (□). Line numbers are indicated to the left of each sampling transect. Black lines with arrows indicate the mean flow pattern during ENSO conditions. SAW: Subarctic Water; StSW: Sub-tropical Surface Water; TSW: Tropical Surface Water

ume of filtered water. The samples were fixed in 4% formalin neutralized with sodium borate. Zooplankton volume (ZV) was obtained via the displacement volume method (Beers 1976). Fish larvae were sorted using a stereoscopic microscope and identified according to Moser (1996). ZV values were standardized to ml per 1000 m^3 of filtered water, and larval abundance was standardized to the number of larvae under 10 m^2 of sea surface (Smith & Richardson 1977).

2.2. Data analysis

A principal component analysis (PCA) was performed using PCOrd V.6 software, to identify which factors determined the environmental variability within each period. PCA was performed on a data matrix consisting of environmental variable measurements at 10 m depth, including SST, sea surface salinity (SSS), and chl *a*. The MLD and ZV were also included. The values of each variable were transformed to the *Z*-score [SE = $X - \mu/\sigma(\sqrt{n} - 1)$], where X = value of the variable X, μ = mean value of the X variables, σ = standard deviation, and n = number of data points. Separate PCAs were done for each year. A multi-response permutation procedure (MRPP) was performed with PCOrd v.6 software to assess if there were statistical differences between the station groups obtained from the PCA. When the within-group homogeneity compared to the random expectation values (A) are below 0.1 ($p < 0.01$), it means that there is a statistically significant difference between them (McCune & Grace 2002).

We assigned the faunistic affinity (tropical, subtropical, or temperate) and adult habitat (epipelagic, demersal, or mesopelagic) of each species according to Eschmeyer et al. (2019) and Froese & Pauly (2019). Basic statistics about the species composition and abundance were separated by region (north and south of PE) for 2 reasons: (1) the PCA of the 3 surveys showed significant environmental differences between regions north and south of PE; and (2) the survey conducted in the fall of 2011 was considerably shorter than those of 2014 and 2015, and the southern region was not comprehensively sampled (only 15 sampling stations in the neritic area of the Gulf of Ulloa).

For the reasons stated above, due to the shorter coverage of the 2011 survey, comparisons of abundance and species composition between the summer 2014 and summer–fall 2015 with the fall of 2011 were made using only 75 equivalent sampling stations among the surveys.

To establish the composition of the fish larval assemblages, a cluster analysis (CA) was carried out with a data matrix formed by the 58 dominant taxa from the 3 surveys. We considered as dominant species those that in total accounted for 98% of the abundance of the period 2011–2015 and/or were present in at least 10% of the stations of each cruise. The CA was performed with PCOrd V.6 software, using the Bray-Curtis similarity index and the simple averaging link method. Groups taken into consideration were those formed with similarity values higher than 0.5. The abundances of the species groups obtained from the CA were plotted on a map, considering only those sampling stations with 2 or more species from the analyzed group.

To establish the effect of the environmental gradients on larval fish distribution and abundance in each period (fall 2011, summer 2014, and summer–fall 2015) and each region (north and south), a canonical correspondence analysis (CCA) was performed, using the same environmental matrix for PCA as the secondary matrix with the variables of SST, SSS, chl *a*, ZV, and MLD. To minimize the differences in the extreme abundance values between species and to reduce the variance, before the CA and CCA, the larval fish abundance was transformed to [log (x_{ij} + 1)], where x is the abundance of taxon i at station j.

3. RESULTS

3.1. Environmental analysis

The cumulative explained variance on the first 3 principal components was higher than 83% in the 3 study years. In all cases, only the physical variables (mainly SST and SSS, but also MLD) had high correlation coefficients with the first component (PC1), except for chl *a* during the fall of 2011 (Table 1). The second component (PC2) had a high correlation primarily with the biological variables chl *a* and ZV (Table 1). PC3 was consistently not highly correlated with any of the variables and was not considered further.

Dispersion diagrams of the PCA showed in all cases 2 main groups of sampling stations on opposite sides of PC1 (Fig. 2). In the case of the fall of 2011 (Fig. 2a), the group on the right side of PC1 corresponds to the southern sampling stations from the Gulf of Ulloa to Bahía Magdalena (transect lines 127 to 140, see Fig. 1), while the group on the left side corresponds to northern sampling stations from PE to Ensenada (lines 123 to 100). Dispersion diagrams for summer of 2014 and summer–fall of 2015 (Fig. 2b,c) showed 2 main sampling station groups: one group from north of Ensenada to PE (lines 97 to 120) and the second group from south of PE to Cabo San Lucas (lines 123 to 153). According to the PCA as well as the MRPP, the environmental characteristics of the northern and southern regions during the fall of 2011 ($A = 0.075$; $p < 0.01$), summer 2014 ($A = 0.091$; $p < 0.01$), and summer–fall of 2015 ($A = 0.048$; $p < 0.01$) had significant differences, suggesting that the area off PE (lines 120 and 123) constitutes a boundary between 2 different environmental systems.

3.2. Water masses and environmental gradients

The T-S diagrams showed that the northern region during the 3 years had a predominance of Subarctic Water (SAW) and Equatorial Subsurface Water (ESsW) (Fig. 2). Transitional water (TrW) increased in the northern region during 2014 and 2015 (Fig. 2b,c) compared with 2011 (Fig. 2a). During the fall of 2011, the southern region (Fig. 2a) had a predominance of SAW, with trace signs of Subtropical Surface Water (StSW). During 2014 and 2015, the SAW was no longer dominant, and warmer and more saline water from the StSW entered the area (Fig. 2b,c).

Results of PCA and T-S diagrams showed that the main environmental gradient was latitudinal. This was evident in the distribution of SST and SSS (Fig. 3a–f), while chl *a* and ZV showed the typical increase from ocean to coast (Fig. 3g–l). The warming of the WBCP from 2011 to 2015 is depicted by the 22°C isotherm, located at the Gulf of Ulloa (~26° N) during the fall of 2011, moving up north of PE (~28° N) during the summer of 2014 and off Ensenada (~30° N) during the summer–fall of 2015 (Fig. 3a–c). Mean SST values during the 3 surveys exhibited a difference of 4.9°C between cooler and warmer years; in the northern region, the value was 18.7°C ($\delta = 1.7$) during the fall of 2011, while it was 21°C ($\delta = 1.8$) during 2014, and 23.6°C ($\delta = 0.9$) during the summer–fall of 2015 (Table 2). This was more evident in the southern region, where the difference between the coolest (21.8°C in 2011) and the warmest year (27.1°C in 2014) was 5.3°C (Table 2).

In the northern region, mean values of chl *a* decreased from 0.22 mg m^{-3} during the fall of 2011 to 0.07 mg m^{-3} in 2015. Meanwhile, ZV changed from

Table 1. Principal component analysis of the environmental variables for fall 2011, summer 2014, and summer–fall 2015. Eigenvectors (EV) were scaled to unit length for each component (PC1–PC3). V%: explained variance; CV%: cumulative explained variance; SST: sea surface temperature; SSS: sea surface salinity; MLD: mixed layer depth; Chl *a*: chlorophyll *a* concentration; ZV: zooplankton volume

					Coefficient of correlation				
		EV	V%	CV%	SST	SSS	MLD	Chl *a*	ZV
Fall 2011	PC1	2.32	46.32	46.32	0.97	0.83	0.56	–0.61	0.10
	PC2	1.17	23.36	69.69	–0.10	–0.37	0.47	–0.36	–0.82
	PC3	0.78	15.55	85.24	–0.14	–0.39	0.09	–0.59	0.50
Summer 2014	PC1	2.91	48.43	0.91	–0.98	–0.94	0.12	0.46	–0.19
	PC2	1.29	21.57	69.99	–0.07	0.02	–0.62	0.62	0.71
	PC3	0.91	15.10	85.10	–0.01	–0.15	–0.76	–0.17	0.08
Summer–Fall 2015	PC1	2.91	48.51	48.51	0.90	0.93	0.63	–0.19	–0.11
	PC2	1.32	22.07	70.58	–0.01	–0.23	0.19	–0.80	–0.76
	PC3	0.76	12.72	83.29	–0.15	0.07	–0.13	0.52	–0.64

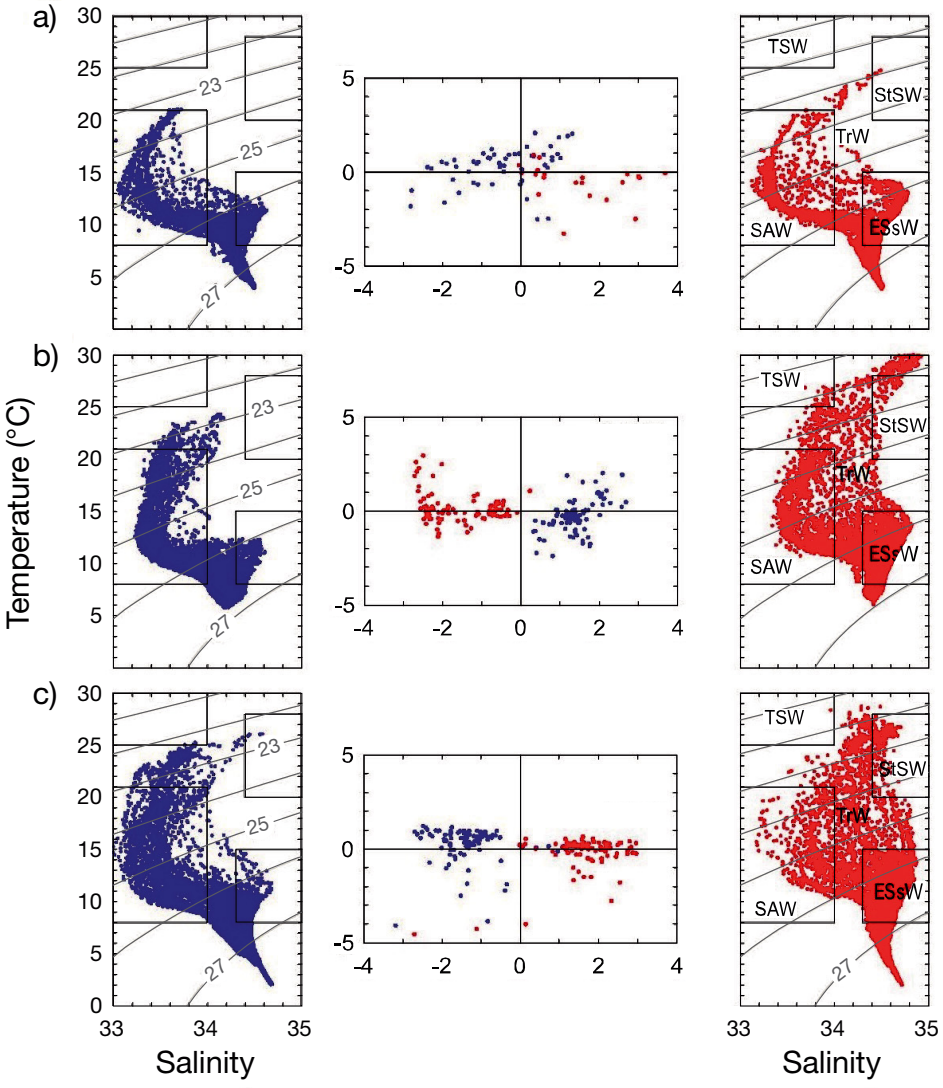

Fig. 2. PCA dispersions for the environmental variables for (a) fall 2011, (b) summer 2014, and (c) summer–fall 2015, each with its respective temperature-salinity diagrams of the northern region (blue dots) and southern region (red dots). TSW: Tropical Surface Water; StSW: Subtropical Surface Water; TrW: Transitional Water; SAW: Subartic Water; ESsW: Equatorial Subsurface Water. Temperature and salinity intervals for each water mass from Durazo & Baumgartner (2002)

174 ml m^{-3} in 2011 to 73.92 ml m^{-3} in 2015 (Table 2), which represents a decrease of 31% in chl *a* and 42% in ZV. In the southern region, ZV values for the same area during the 3 surveys had a higher change in 2015, with a decrement of 64% between LN 2011 and EN 2015 (Table 2).

The lowest MSLAs (–10 cm) were found during the fall of 2011, mainly in the northern region, increasing to an average of 10 cm in the summer of 2014, with higher values in the coastal area to the south of PE, and from 20 to 40 cm in almost all areas between Cabo San Lucas and Ensenada during the summer–fall of 2015 (Fig. 4).

3.3. Geostrophic flow

The geostrophic flow during the fall of 2011 showed the strongest currents in a southward direction across 3 cyclonic eddies located off Ensenada, between Bahía Sebastián Vizcaíno and PE (~29–27° N) and a third one located at the Gulf of Ulloa (Fig. 4a). A weak poleward flow went near the coast until line 123, south of PE (Fig. 4a). During the summer of 2014, a coastal and northward geostrophic flow was interrupted off PE by 2 cyclonic eddies. The northward flow was diverted west, heading south again, along with a series of meanders and eddies, of

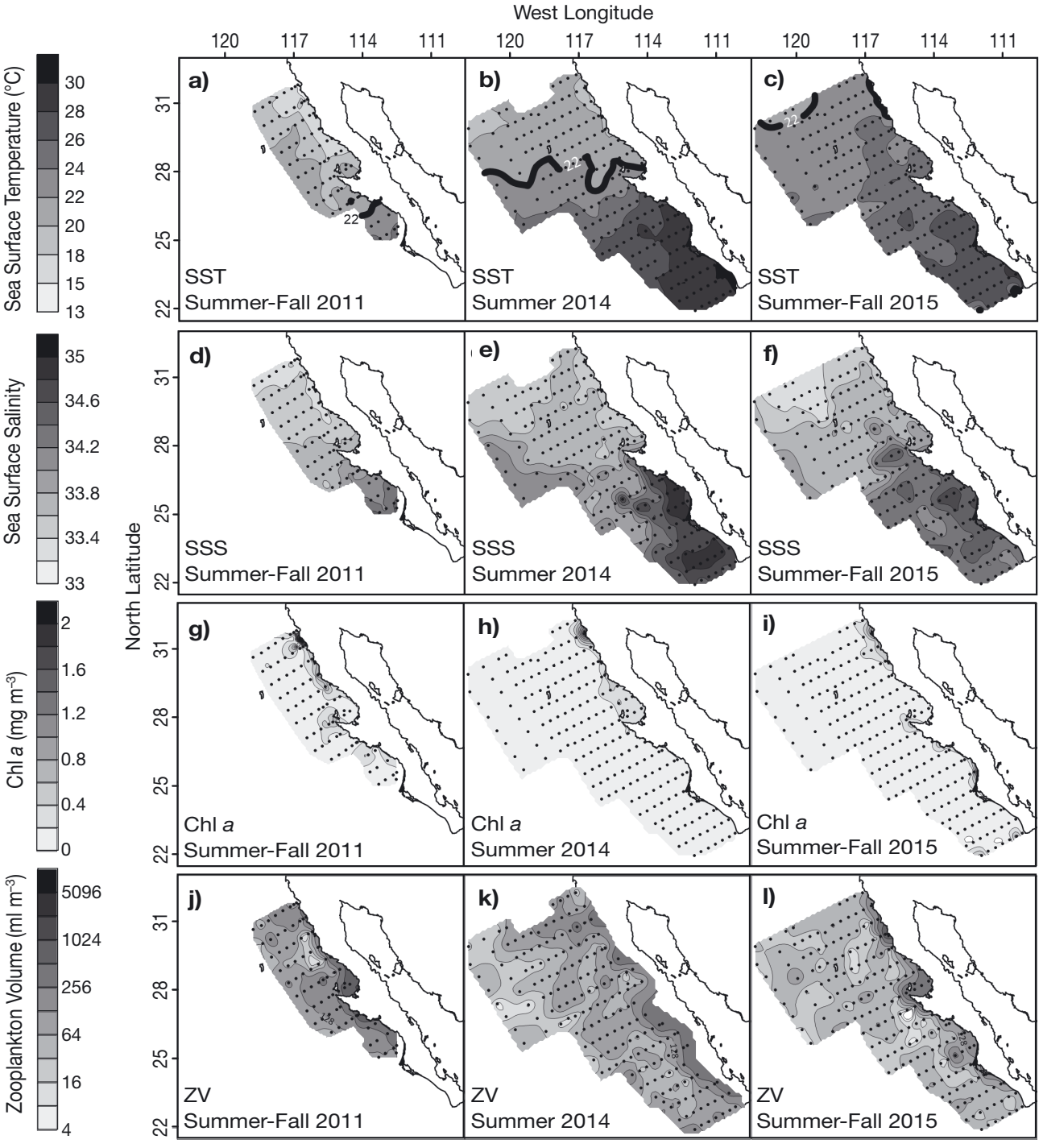

Fig. 3. Sea surface distribution of (a–c) temperature, (d–f) salinity, (g–i) chl *a* concentration, and (j–l) zooplankton volume (ZV) during fall 2011 (left column), summer 2014 (center column), and summer–fall 2015 (right column). Black lines in panels a–c represent the 22°C isotherm

which the most intense was located between 22 and 23°N (Fig. 4b). North of PE, there was still a northward coastal flow, although lower in intensity than the one observed south of PE; concurrently, and associated with it, there was a system of alternating cyclonic and anticyclonic eddies, while there was an ocean-ward flow off Punta Baja and Ensenada (Fig. 4b). In the summer–fall of 2015, the coastal poleward flow was stronger and wider, and it was observed northward as far as Ensenada (Fig. 4c). Three

Table 2. Mean and SD of sea surface temperature (SST), chlorophyll *a* concentration (Chl *a*), and zooplankton volume (ZV) for fall 2011, summer 2014, and summer–fall 2015 in the northern (NR) and southern (SR) regions. Values for the 2014 and 2015 surveys were calculated for the same sampling area as the 2011 survey

		SST (°C)	SD	Chl *a* (mg m^{-3})	SD	ZV (ml 1000 m^{-3})	SD
Fall 2011	NR	18.7	1.7	0.22	0.28	174.78	198.33
	SR	21.8	1.8	0.15	0.08	239.62	228.22
Summer 2014	NR	21.0	1.8	0.18	0.27	81.32	81.71
	SR	27.1	2.1	0.09	0.02	162.38	131.96
Summer–Fall 2015	NR	23.6	0.9	0.07	0.12	73.92	124.21
	SR	26.0	1.4	0.08	0.05	85.39	91.41

cyclonic eddies were detected. The most intense was near 30°N, while 2 of lower intensity were in the oceanic region off the Gulf of Ulloa and off the southern end of the peninsula (Fig. 4c). An anticyclonic eddy also occurred in the oceanic region at 27°N (Fig. 4c).

3.4. Description of the larval fish community

The larval fish community of the WBCP comprised 421 taxa in 22 orders, 104 families, and 213 genera during the 2011–2015 period. Only 58 taxa were abundant and/or frequent in at least 1 of the 3 surveys, and together they accounted for 98% of the total abundance (Table 3). Nine species (6 mesopelagic and 3 demersal) accounted for 90–97% of the total abundance throughout the 3 surveys. The mesopelagic species *Vinciguerria lucetia*, *Diogenichthys laternatus*, and *Triphoturus mexicanus* were always the most abundant species. Although considered frequent during the 3 surveys, *Cyclothone signata*, *Bathylagoides wesethi*, and *Ceratoscopelus townsendi* were only abundant during the warm period between 2014 and 2015 (Table 3). The mesopelagic *Benthosema panamense*, *Scopelogadus mizolepis*, and *Argyropelecus sladeni*, the epipelagic *Auxis* spp., and the demersal *Ctenogobius sagittula* and *Bregmaceros* sp. 1 were only present during the warm period in the summer of 2014 and the summer–fall of 2015 (Table 3). The demersal species *Synodus lucioceps*, *Prionotus stephanophrys*, and *Citharichthys stigmaeus* were only abundant during the fall of 2011 (Table 3).

In the northern region, the mean larval abundance calculated for the same area for the 3 surveys de-

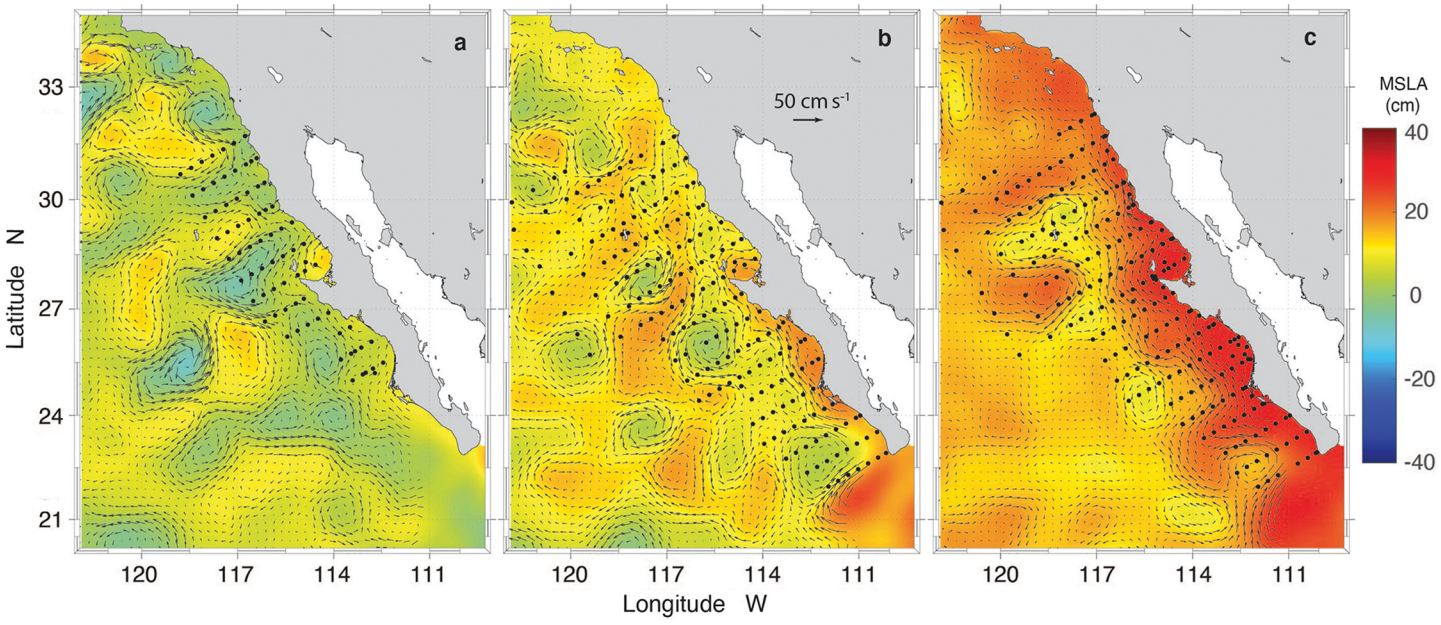

Fig. 4. Mean sea level anomaly (MSLA; color scale) and geostrophic flow (arrows) during (a) fall 2011, (b) summer 2014, and (c) summer–fall 2015

Table 3. Total abundance (TAB), relative abundance (AB%), and frequency (F%) of the most abundant and frequent fish larvae collected during fall 2011, summer 2014, and summer–fall 2015. Gray shading corresponds to those species that together accounted for 85% of the abundance or were present in at least 10% of the sampling stations in each survey; empty cells: abscence of the species in the respective survey

Taxon	Fall 2011			Summer 2014			Summer–fall 2015		
	TAB	AB%	F%	TAB	AB%	F%	TAB	AB%	F%
Meso-bathypelagic									
Bathylagoides wesethi	730	1.45	48	4574	4.05	48	1976	2.38	40
Nansenia crassa	3	0.01	1	120	0.11	11	65	0.08	7
Cyclothone signata	288	0.57	36	994	0.88	37	1991	2.4	46
Cyclothone acclinidens	58	0.12	9	786	0.7	26	514	0.62	23
Argyropelecus sladeni				199	0.18	14	112	0.13	15
Argyropelecus affinis	7	0.01	1	143	0.13	13	42	0.05	3
Vinciguerria lucetia	13029	25.82	87	68488	60.67	95	46066	55.53	93
Ichthyococcus irregularis	36	0.07	13	121	0.11	9	94	0.11	8
Stomias atriventer	86	0.17	13	119	0.11	10	203	0.24	19
Scopelogadus mizolepis				131	0.12	9	252	0.3	36
Lestidiops ringens	132	0.26	27	28	0.02	3	46	0.06	5
Diogenichthys laternatus	1549	3.07	55	9101	8.06	80	8626	10.4	76
Triphoturus mexicanus	4128	8.18	85	10804	9.57	72	4121	4.97	57
Ceratoscopelus townsendi	44	0.09	11	1685	1.49	26	931	1.12	23
Protomyctophum crockeri	111	0.22	23	738	0.65	38	660	0.8	35
Lampadena urophaos	27	0.05	5	585	0.52	19	357	0.43	23
Lampanyctus idostigma	68	0.13	17	74	0.07	6	471	0.57	23
Hygophum reinhardtii	3	0.01	1	42	0.04	4	568	0.68	22
Hygophum atratum	58	0.12	4	240	0.21	13	292	0.35	13
Notoscopelus resplendens	26	0.05	7	428	0.38	24	100	0.12	8
Benthosema panamense				15	0.01	2	531	0.64	15
Gonichthys tenuiculus	64	0.13	7	224	0.2	17	176	0.21	16
Myctophum nitidulum	42	0.08	11	167	0.15	12	234	0.28	21
Diogenichthys atlanticus	37	0.07	9	126	0.11	6	243	0.29	14
Symbolophorus californiensis	143	0.28	31	72	0.06	6	116	0.14	12
Lampanyctus ritteri	50	0.1	13	87	0.08	8	27	0.03	2
Diaphus theta	68	0.13	11	73	0.06	4			
Melamphaes lugubris	108	0.21	24	175	0.15	14	106	0.13	11
Chiasmodon niger	13	0.03	4	192	0.17	15	167	0.2	13
Cubiceps pauciradiatus	6	0.01	1	106	0.09	4	444	0.54	12
Coastal pelagic									
Sardinops sagax	1150	2.28	28	294	0.26	10	3	0.003	1
Engraulis mordax	147	0.29	12	276	0.24	9	226	0.27	3
Scomber japonicus	101	0.2	15	25	0.02	3			
Epipelagic									
Trachurus symmetricus	267	0.53	10	39	0.03	3			
Coryphaena hippurus	76	0.15	4	50	0.04	4	92	0.11	14
Auxis spp.				452	0.4	12	114	0.14	8
Demersal									
Synodus lucioceps	12100	23.98	31	125	0.11	6	915	1.46	12
Bregmaceros sp. 1				30	0.03	2	384	0.46	26
Ophidion scrippsae	1382	2.74	15	42	0.04	2	117	0.14	4
Lepophidium negropinna	253	0.5	13	67	0.06	4	745	0.9	6
Chilara taylori	84	0.17	15	21	0.02	1	4	0.005	1
Scorpaena guttata	68	0.13	16	46	0.04	4	4	0.004	1
Sebastes sp. 2	69	0.14	13	23	0.02	3			
Prionotus stephanophrys	7002	13.87	17	1931	1.71	7	798	0.96	10
Pronotogrammus multifasciatus	1108	2.2	17	332	0.29	10	268	0.32	9
Chromis punctipinnis	57	0.11	13	770	0.68	15	152	0.18	7
Halichoeres semicinctus	150	0.3	19	61	0.05	3	170	0.2	10
Rhinogobiops nicholsii	133	0.26	15	176	0.16	11	202	0.24	6
Ctenogobius sagittula							476	0.57	23
Citharichthys stigmaeus	2597	5.15	48	242	0.21	12	9	0.01	1
Citharichthys fragilis	295	0.59	17	128	0.11	2	11	0.01	1
Citharichthys sordidus	204	0.4	15	21	0.02	3	5	0.01	1
Citharichthys xanthostigma	98	0.19	16	24	0.02	2			
Hippoglossina stomata	62	0.12	17	8	0.01	1	10	0.01	2
Syacium ovale	26	0.05	10				249	0.30	20
Bothus leopardinus	73	0.14	9	33	0.03	3	88	0.11	11
Symphurus atricaudus	657	1.30	39	44	0.04	2	156	0.19	4
		97.53			93.87			90.58	

Table 4. Total abundance (TAB) by region: north (N) and south (S) for fall 2011, summer 2014, and summer–fall 2015. N: number of samples; MAB: mean abundance of organisms per 10 m^2; Taxa: number of taxa; Dom: number of dominant species; MZV: mean zooplankton volume (ml per 100 m^3); Tr-Str (Tm-Str): number of species with tropical–subtropical (temperate–subtropical) affinity: WD: widely distributed species. Values in the NE and SE columns were calculated for the same north (NE) and south (SE) sampling areas as in the 2011 survey

	Fall 2011			Summer 2014					Summer–Fall 2015				
	Total	N	S	Total	N	S	NE	SE	Total	N	S	NE	SE
N	75	59	16	185	97	88	47	15	188	101	87	49	15
TAB	50467	30389	20078	112893	86362	26531	41447	4586	82962	47434	35528	13035	3381
MAB	673	515	1255	603	890	301	398	305	437	469	408	136	225
Taxa	118	75	81	281	133	211	104	117	259	138	198	96	91
Dom	8	4	6	6	4	23	4	27	15	7	20	6	26
MZV	193	173	266	96	80	111	111	149	66	74	56	101	77
Relative abundance%													
Tr-Str	66.8	59.7	77.5	77.2	75.2	83.6	85.8	93.5	82.1	73.8	93	81.7	84.0
Tm-Str	33.0	40.0	22.4	6.9	8.3	2.7	13.5	5.2	4.9	7.1	2	17.7	7.6
WD	0.2	0.3	0.1	15.9	16.5	13.7	0.7	1.3	13	19.1	5	0.7	8.4
Number of species n													
Tr-Str	65	30	54	178	60	149	40	88	165	70	140	44	67
Tm-Str	45	38	23	42	34	26	52	20	31	25	20	42	15
WD	8	7	4	61	39	36	12	9	63	42	37	10	9

creased by almost 74% from the fall of 2011 (515 ind. 10 m^{-2}) to the summer–fall of 2015 (136 ind. 10 m^{-2}). However, the most significant change in the mean larval abundance was in the southern region, decreasing 82% between 2011 (1255 ind. 10 m^{-2}) and 2015 (225 ind. 10 m^{-2}) (Table 4). The number of taxa increased from 2011 to 2015 in both southern and northern regions. However, the number of dominant species remained almost the same in the northern region during the 3 years (4 to 6 species), while in the southern region, there were 6 dominant species during 2011 in contrast with 27 and 26 dominant species during 2014 and 2015 (Table 4). In addition, in the 3 surveys, the species richness increased in both regions by almost 28% from the cooler to the warmer period (Table 4).

Relative abundance of tropical–subtropical vs. temperate–subtropical taxa was similar in the northern region during the fall of 2011 (59.7 and 40%, respectively), whereas significant differences were found during the summer of 2014 (85.8 vs. 13.5%) and the summer–fall of 2015 (81.7 vs. 17.7%) (Table 4). In the southern region, the difference in the relative abundance between taxa with warm temperature affinity against taxa with cold affinity was distinctively greater; the difference was 77.5 vs. 22.4% during the fall of 2011, 93.5 vs. 5.2% during the summer of 2014, and 84 vs. 7.6% in the summer–fall of 2015 (Table 4). The relative abundance of tropical–subtropical species from the cold to the warm period changed from 59.7 to 85.8% in the north, and from 77.5 to 93.5% in the south, while that of temperate species decreased from 40 to 13.5% in the north and from 22.4 to 5.2% in the south (Table 4).

The number of tropical–subtropical species within the equivalent areas analyzed increased from 2011 to 2015 by 47% in the north (from 30 species in fall 2011 to 44 in summer–fall 2015) and to a maximum of 63% in the south (from 54 in fall 2011 to 88 in summer 2014) (Table 4). Likewise, the number of taxa with cold affinity in the northern region increased from 38 species in the fall of 2011 to a maximum of 52 species in the summer of 2014, but decreased from 23 to 15 species in the south (Table 4).

The relative abundance by habitat showed important changes (Table 5). During 2011 in the northern region, demersal vs. meso- and bathypelagic species almost had the same abundance (45.3 vs. 51.8%); in contrast, during the summer and fall of 2014 and 2015, the meso- and bathypelagic species notably increased their relative abundance to 92.5 and 88.1% while demersal taxa decreased (3.2% in 2014 and 9.8% in 2015). In opposition to the northern region, in the southern region during the fall of 2011, the abundance of demersal taxa was higher than that of meso- and bathypelagic taxa (66.6 vs. 26.8%) (Table 5), but it remained similar during the summer of 2014 (52.3 and 41.9%) and summer–fall of 2015 (47.3 vs. 49.3%).

Demersal species were always the most diverse in the southern region, and meso- and bathypelagic taxa were more diverse in the northern region (Table 5). While species richness of demersal taxa increased

Table 5. Number of demersal (Dem), meso- and bathypelagic (M-B), coastal epipelagic (CE), and oceanic epipelagic species (OE). Values in the NE and SE columns were calculated for the same north (NE) and south (SE) sampling areas as in the 2011 survey

	Fall 2011			Summer 2014					Summer–Fall 2015				
	Total	N	S	Total	N	S	NE	SE	Total	N	S	NE	SE
Relative abundance%													
Dem	53.6	45.3	66.1	6.4	1.8	21.6	3.2	52.3	9.3	6.1	13.7	9.8	47.3
M-B	41.8	51.8	26.8	90.4	96	72	92.5	41.9	88.3	93	81.8	88.1	49.3
CE	2.8	1.8	4.3	2.5	2.1	3.8	3.5	4.6	1.5	0.8	2.6	1.7	0.5
OE	1.8	1.1	2.9	0.7	0.1	2.5	0.8	1.2	0.9	0.1	1.9	0.5	3.0
Number of species n													
Dem	64	28	52	150	43	128	38	85	136	47	115	39	63
M-B	38	34	19	87	70	52	50	21	92	79	58	52	20
CE	4	3	3	33	15	23	8	6	18	4	16	2	3
OE	12	10	7	11	5	8	8	5	13	7	8	3	5

from the cool to the warm period, meso- and bathypelagic taxa remained almost the same during the 3 years, ranging from 34 to 52 taxa in the northern region, and from 19 to 21 in the southern region (Table 5).

3.5. Fish larval assemblages

The CA showed 11 larval assemblages with a similarity level higher than 50% (Fig. 5). These groups showed 4 general distribution patterns (Fig. 6):

(1) Wide distribution assemblage (WD). Three mesopelagic species formed the WD oceanic assemblage, 2 of which have a subtropical affinity (*D. laternatus* and *T. mexicanus*) and *B. wesethi* with temperate-subarctic affinity (Fig. 5). WD had its lowest abundance during 2011 with a more oceanic distribution (Fig. 6a). During 2014, its abundance increased toward the coast in the northern region, and during 2015, its highest abundance was in the north oceanic region, decreasing substantially off the mid-region of the peninsula (Fig. 6b,c).

(2) Northern complex assemblages. Six assemblages formed this species complex, of which 2 were exclusively formed by mesopelagic species (Fig. 5) with a northern oceanic distribution, increasing their abundance from 2011 to 2015 (Fig. 6d–f; Fig. S1a,b in the Supplement at www.int-res.com/articles/suppl/m14331_supp.pdf). The mesopelagic assemblage 1 (NO1) was formed by *C. signata, Protomyctophum crockeri, C. townsendi, Cyclothone acclinidens, Myctophum nitidulum, Lampadena urophaos* (with temperate and/or subarctic affinity), *Gonichthys tenuiculus* (subtropical–tropical), and *Notoscopelus resplendens* (wide distribution). NO2 included *Stomias atriventer, Chiasmodon niger* (temperate–subarctic), *Diogenichthys atlanticus*, and *S. mizolepis* (wide distribution).

Four northern groups had coastal distributions. NC1 consisted of the demersal species *C. stigmaeus*, *Paralabrax maculatofasciatus* (subtropical), *Chilaria taylori* (temperate–subtropical), *Sebastes* sp. 2, and the subarctic–temperate species *Lestidiops ringens*, which was abundant during 2011 but not detected during 2015 (Fig. S1d–f). NC2 was composed of temperate–subtropical coastal pelagic *Sardinops sagax*, *Engraulis mordax*, and *Scomber japonicus*; the demersal *Syngnathus californiensis, Citharichthys xanthostigma*, and *Bregmaceros bathymaster*; and the mesopelagic *Diaphus theta* and *Symbolophorus californiensis*. The distribution of NC2 was between Ensenada and Bahía Magdalena in 2011 and 2014, and only at 2 sampling stations off Ensenada during 2015 (Fig. S1g–i). A third northern coastal assemblage (NC3) was formed by temperate–subtropical species, 2 of them demersal (*Chromis punctipinnis* and *Rhinogobiops nicholsii*) and 2 mesopelagic (*Melamphaes lugubris* and *Nansenia crassa*) (Fig. 5), which were mainly distributed north of PE and were more abundant during 2014 (Fig. S1j–l). In addition, NC4 was formed by the epipelagic *Trachurus symmetricus* and demersal *Symphurus atricauda*, with temperate–subtropical affinity, and was found between Punta Banda and Bahía Magdalena. Its highest abundance was during the fall of 2011, and it was not detected during 2015 (Fig. S2a–c).

(3) Southern complex assemblages. The southern region had 3 species groups: 1 oceanic and 2 coastal (Fig. 5). SO1 was formed by southern species from warm waters: 6 meso-bathypelagic species (*D. pacificus*, *Hygophum atratum*, *B. panamense, Cubiceps pauciradiatus*, *Lestidiops neles*, and *Lampanyctus idostigma*) as well as 1 deep demersal (*Bregmaceros*

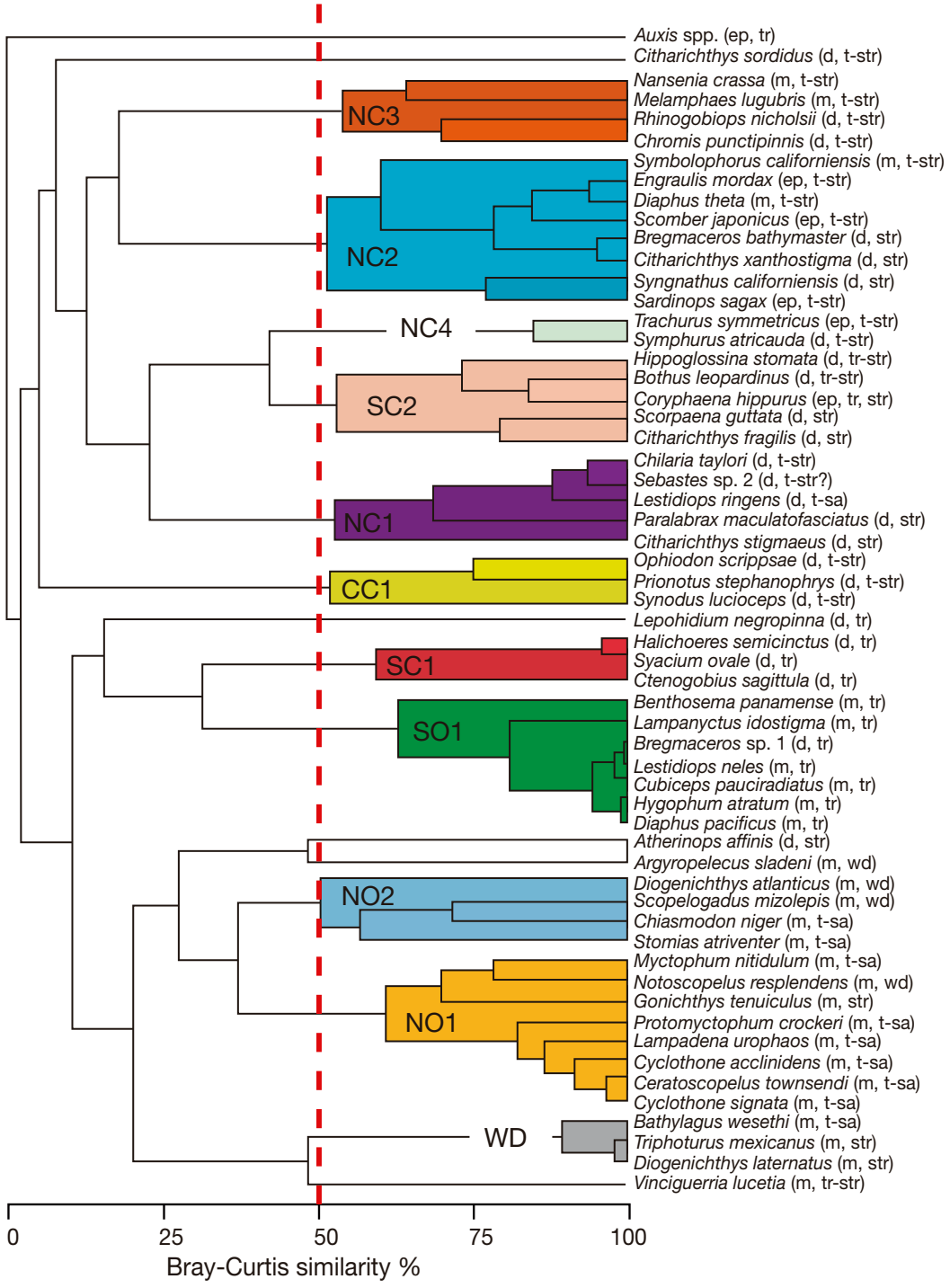

Fig. 5. Fish larval assemblages with a similarity level higher than 50% (indicated by the red dashed line) during the summer–fall period of 2011 and 2014–2015. WD: wide distribution; NO1: north oceanic 1; NO2: north oceanic 2; SO1: south oceanic 1; SC1: south coastal 1; SC2: south coastal 2; CC1:central coastal 1; NC1: north coastal 1; NC2: north coastal 2; NC3: north coastal 3; NC4: north coastal 4; ep: epipelagic; tr: tropical; d: demersal; t: temperate; str: subtropical; m: mesopelagic; sa: subarctic; wd: wide distribution

sp. 1). The highest abundance of SO1 was during 2015, south of Bahía Magdalena (Fig. 6g–i). Group SC1, with species from neritic waters with tropical affinity (*C. sagittula*, *Syacium ovale*, and *Halichoeres semicinctus*), was found toward the Gulf of Ulloa during 2011 and 2014 but extended its distribution along the coast during 2105 from Cabo San Lucas to Ensenada (Fig. S2d–f). Group SC2 was composed of the

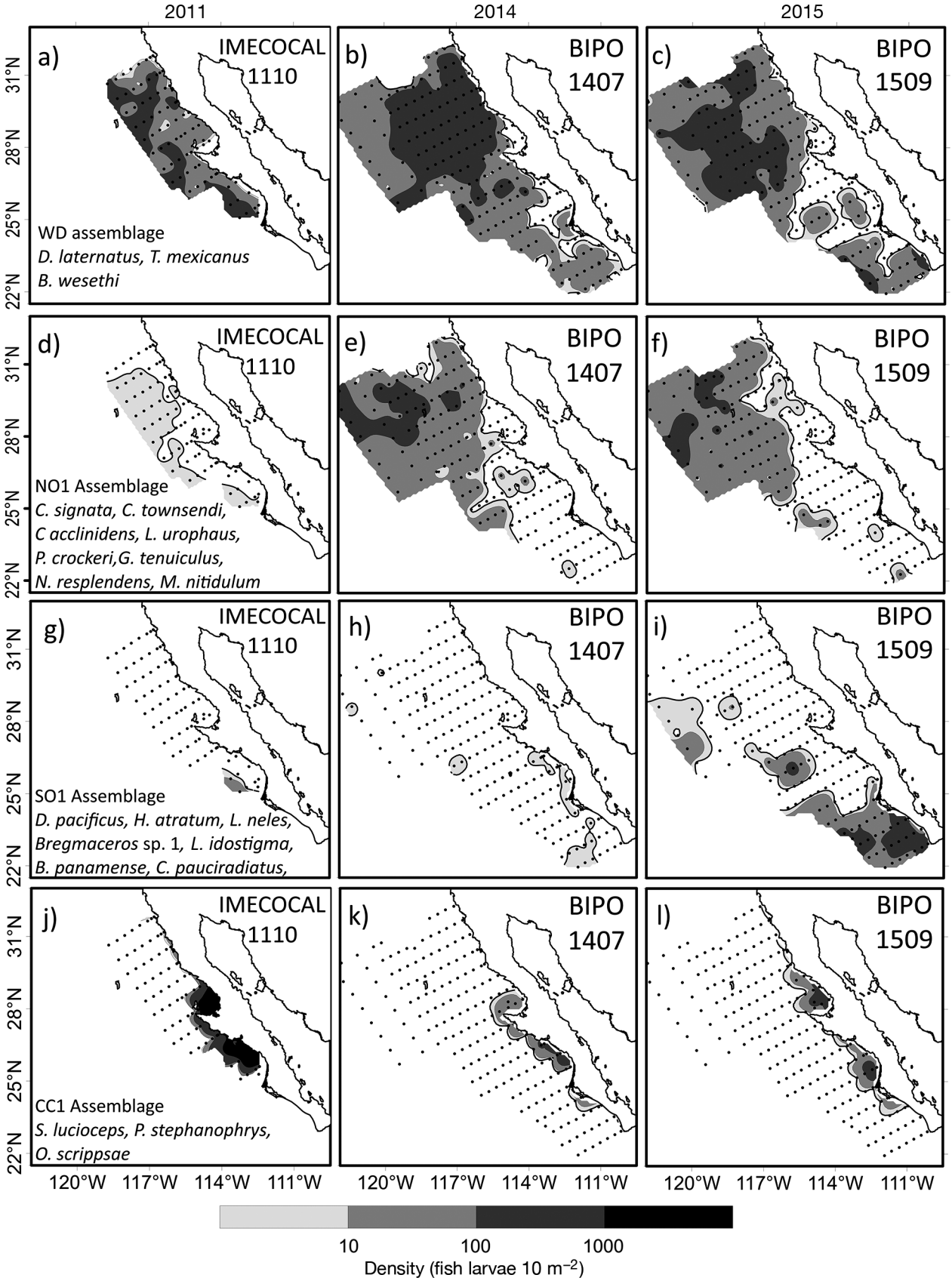

Fig. 6. Distribution of the fish larval assemblages during the summer–fall seasons of 2011 and 2014–2015. Assemblage abbreviations and complete species names are given in Fig. 5; numbers in the top right corners refer to the cruises (see Section 2.1 for details)

demersal *Bothus leopardinus* (tropical–subtropical), *Citharichthys fragilis, Hippoglossina stomata*, and *Scorpaena guttata* (all of them with subtropical affinity) and the epipelagic *Coryphaena hippurus* (tropical–subtropical) distributed from Punta Banda to Cabo San Lucas (Fig. S2g–i).

(4) Central assemblage. The central coastal assemblage CC1 (Fig. 5) was composed of 3 demersal species with temperate–subtropical affinity (*S. lucioceps*, *P. stephanophrys*, and *Ophiodon scrippsae*), and was present toward Bahía Sebastián Vizcaíno and the Gulf of Ulloa at all sapling times. Its highest abundance was during the fall of 2011, but its widest distribution was during the summer–fall of 2015, from Bahía Magdalena to Ensenada (Figs. 6j–l).

3.6. Environment vs. larval fish distribution

The CCA showed that the environmental variables determining the distribution of fish larvae were different, depending on the region (north or south of PE) and the year (Table 6). During the fall of 2011, in the north, the first 3 axes explained 26.4% of the variance, while in the south, 34.4% of the variance was explained (the highest explained variance of the 3 surveys). During the summer of 2014, the explained variance was 18% in the north and 23.9% in the south, whereas in 2015, the variance explained by the first 3 axes was greater in the northern region (26.2%) than in the southern region (18.1%). The number of variables with a correlation value above 0.5 with axis 1 was greater during 2014 (4 in the northern region and 3 in the southern region) than in 2015 (2 variables in both regions).

During the fall of 2011, in the northern region, only ZV had a high correlation value with axis 1 (R^2 = 0.91), while on axis 2, the highest correlation values were with the physical variables SST (R^2 = 0.98) and SSS (R^2 = 0.72). The dispersion diagram for the northern region showed that demersal species *C. xanthostigma*, *P. stephanophrys*, *O. scrippsae, M. lugubris, S. japonicus*, and *S. lucioceps* were associated with high ZV values, and *S. californicus*, *C. stigmaeus*, and *P. crockeri* were associated with high chl *a* values (Fig. 7a). In the southern region, the biological variables chl *a* (R^2 = −0.71) and ZV (R^2 = −0.64) were also those with the highest correlation values on axis 1 (Table 6), and the physical variables SST (R^2 = −0.94) and SSS (R^2 = −0.98) had the highest R^2 values on axis 2. Demersal species such as *C. xanthostigma*, *P. stephanophrys*, *O. scrippsae*, *S. lucioceps*, and

Table 6. Canonical correspondence analyses for the northern and southern region during 2011, 2014, and 2015. EGV: eigenvalue; EV%: explained variance; CEV%: cumulative explained variance. Also shown are Pearson correlations between species and environment matrices (Sp/Env), and correlation values for each of first 3 axes with: mixed layer depth (MLD), sea surface temperature (SST), sea surface salinity (SSS), chlorophyll *a* concentration (Chl *a*), and zooplankton volume (ZV). Values in **bold** are those above ±0.5

	Fall 2011			Summer 2014			Summer-fall 2015		
	Axis 1	Axis 2	Axis 3	Axis 1	Axis 2	Axis 3	Axis 1	Axis 2	Axis 3
Northern Region									
EGV	0.37	0.20	0.08	0.23	0.05	0.040	0.29	0.09	0.05
EV%	15.2	8.1	3.2	12.7	3.0	2.3	17.7	5.3	3.2
CEV%	15.2	23.3	26.4	12.7	15.7	18.0	17.7	23.1	26.2
Sp/Env	0.89	0.85	0.63	0.82	0.77	0.65	0.79	0.76	0.62
MLD	−0.26	**−0.55**	−0.01	−0.34	0.09	0.24	−0.19	0.31	0.42
SST	0.08	**−0.98**	0.18	**−0.63**	**−0.56**	−0.49	0.18	**0.95**	0.09
SSS	0.36	**−0.72**	0.41	**−0.54**	**−0.66**	−0.18	0.15	**0.76**	0.06
Chl *a*	0.35	**0.53**	−0.29	**0.92**	−0.26	0.19	**0.60**	0.05	−0.48
ZV	**0.91**	−0.06	0.01	**0.56**	**0.52**	−0.48	**0.97**	−0.14	0.17
Southern Region									
EGV	0.32	0.20	0.13	0.49	0.15	0.12	0.30	0.15	0.06
EV%	16.7	10.7	7.1	15.5	4.6	3.8	10.9	5.3	2.0
CEV%	16.7	27.4	34.4	15.5	20.1	23.9	10.9	16.2	18.1
Sp/Env	0.91	0.85	0.86	0.89	0.80	0.76	0.80	0.78	0.63
MLD	0.11	−0.14	−0.24	0.40	0.34	−0.22	−0.04	0.29	0.40
SST	0.24	**−0.94**	0.15	**0.65**	**0.65**	−0.09	0.01	−0.41	0.06
SSS	−0.01	**−0.98**	−0.01	**0.81**	0.49	−0.19	**−0.67**	**−0.51**	0.48
Chl *a*	**−0.71**	0.11	−0.02	0.37	−0.02	0.44	−0.09	−0.23	−0.05
ZV	**−0.64**	−0.08	0.15	**−0.77**	−0.49	0.30	**−0.76**	0.01	−0.49

B. bathymaster were associated with high ZV values, while *B. leopardinus*, *S. atricauda*, *H. semicinctus*, and *Pronotogrammus multifasciatus* were associated with low ZV values (Fig. 7b).

In the summer of 2014, in the northern region, the physical variables SST and SSS, and particularly the biological variable chl *a* (which had the highest correlation value; $R^2 = 0.92$) determined the distribution of fish larvae (Table 6). The scatter plot in Fig. 8a shows coastal neritic species associated with high chl *a* values (*S. sagax*, *E. mordax*, *C. stigmaeus*, *C. punctipinnis*, *R. nicholsii*) separated from 3 different groups of mesopelagic species that responded differently to environmental gradients. The first group was composed of mesopelagic species associated with high SST and SSS values (*D. atlanticus*, *D. laternatus*, *Argyropelecus affinis, C. signata. M. lugubris*, and *A. sladeni*). The second mesopelagic group was composed of cold-habitat species that were associated with low SST values and high ZV values (*S. californiensis*, *N. crassa, S. californiensis*, and *L. ritteri*), and the third group was associated with low chl *a* values (*C. townsendi*, *S. bispinosus, P. crockeri, M. nitidulum*, *B. wesethi*). In the southern region, SST, SSS, and ZV were the variables with the greatest weight on axis 1 (Table 6). These variables separated demersal and epipelagic taxa associated with higher SSS and SST (*Syacium* spp., *Ophicthus zophochir, Caranx caballus*, *Auxis* spp., and *Opisthonema* spp., among others) from mesopelagic species (*A. sladeni*, *C. niger*, *P. crockeri*, and *B. wesethi*, among others) associated with areas of higher concentration of ZV (Fig. 8b).

Over the summer–fall of 2015, the species distribution in the north was defined on axis 1 only by the biological variables (Table 6), which determined a division between demersal species associated with high ZV and chl *a* values in the coastal region (*S. lucioceps* and *C. punctipinnis*), and the rest of the mesopelagic species with oceanic distribution (Fig. 9a). The fish larval distribution in the southern region was primarily determined on axis 1 by ZV and SSS (Table 6). SST had a high correlation with the northern region only in axis 2. Fig. 9b shows the separation of the neritic species, mainly demersal, associated with high SSS values (*Syacium* spp., *B. leopardinus*, *H. semicinctus*, *P. multifasciatus*, *S. lucioceps*, *C. hippurus*, *Serranus* sp., among others) from mesopelagics, associated with low SSS (*B. wesethi*, *L. urophaos*, *C. signata*, and *T. mexicanus*) or low ZV values (*H. atratum*, *Diplophos* sp. 1, and *L. neles*). Chl *a* was not correlated with the fish larval distribution south of PE in either of the surveys (2014 and 2015).

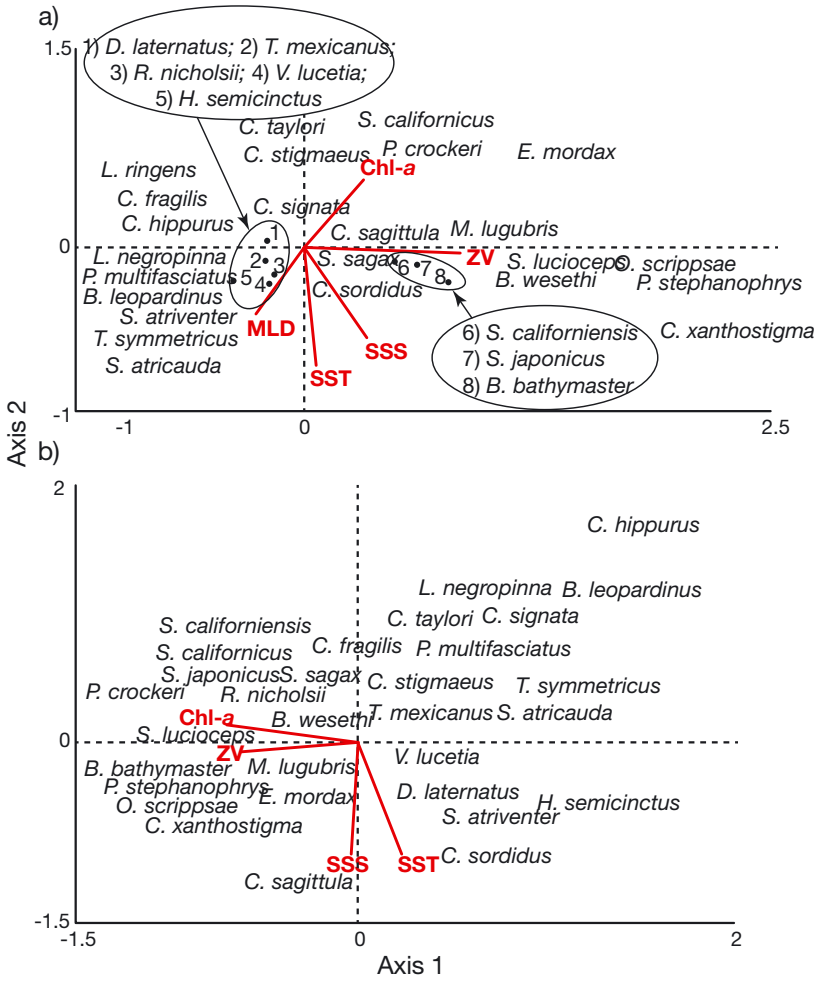

Fig. 7. Species dispersion diagrams from canonical correspondence analysis (CCA) during fall 2011 (cruise IMECOCAL-1110) in (a) the northern region (N) and (b) the southern region (S). MLD: mixed layer depth; SST: sea surface temperature; SSS: sea surface salinity; ZV: zoo-plankton volume; Chl-a: chl *a*

4. DISCUSSION

4.1. Environmental scenario

The WBCP central region off PE is a transition zone of high larval fish diversity (Jiménez-Rosenberg et al. 2020) where the southern tropical–subtropical com-

munity meets the northern temperate–subarctic, and the local fish community of Bahía Sebastián Vizcaíno (Moser & Smith 1993). The region remained as a transitional zone during the 3 analyzed periods, since the PCA established 2 zones differentiated by their oceanographic characteristics in which the boundary between them was off the PE region. In this area, several species have their latitudinal distribution limit associated with the latitudinal environment gradients (Aceves-Medina et al. 2019). Thus, the study of fish larval distribution during the warm seasons of 2011, 2014, and 2015 allowed us to track the effects caused by the advance and retreat of the different water masses that converged there during LN, EN, and The Blob processes.

The propagation of interannual signals changed between both northern and southern regions of the WBCP, and it determined biological differences in response to water masses (Durazo et al. 2010). On this time scale, the environmental data showed the transition from cold conditions in 2011, dominated by SAW low temperatures and a dominant southward geostrophic flow, and then shifting to anomalously warm conditions in 2015, where the geostrophic flow was predominantly coastal and northward, carrying warm oligotrophic waters as far as Ensenada. In a broad context, these environmental conditions were happening within a cool period (1998 to 2013) of the Pacific Decadal Oscillation (PDO), which reached the lowest negative values in the fall of 2011, coinciding with the strong 2011–2012 LN event. Following this, during the winter of 2014, a rapid shift to PDO positive anomalies started that reached its highest values during EN 2015–2016.

In the fall of 2011, the greatest thermal change was observed south of PE, where the thermal anomalies reached –5°C, while at the north, the values were at –2°C (Bjorkstedt et al. 2012, Zaitsev et al. 2014). This 3°C difference between the northern and southern regions during 2011 contrasted with a difference of 6.1°C registered between both regions during the summer of 2014, even greater than during the summer–fall of 2015 (2.4°C).

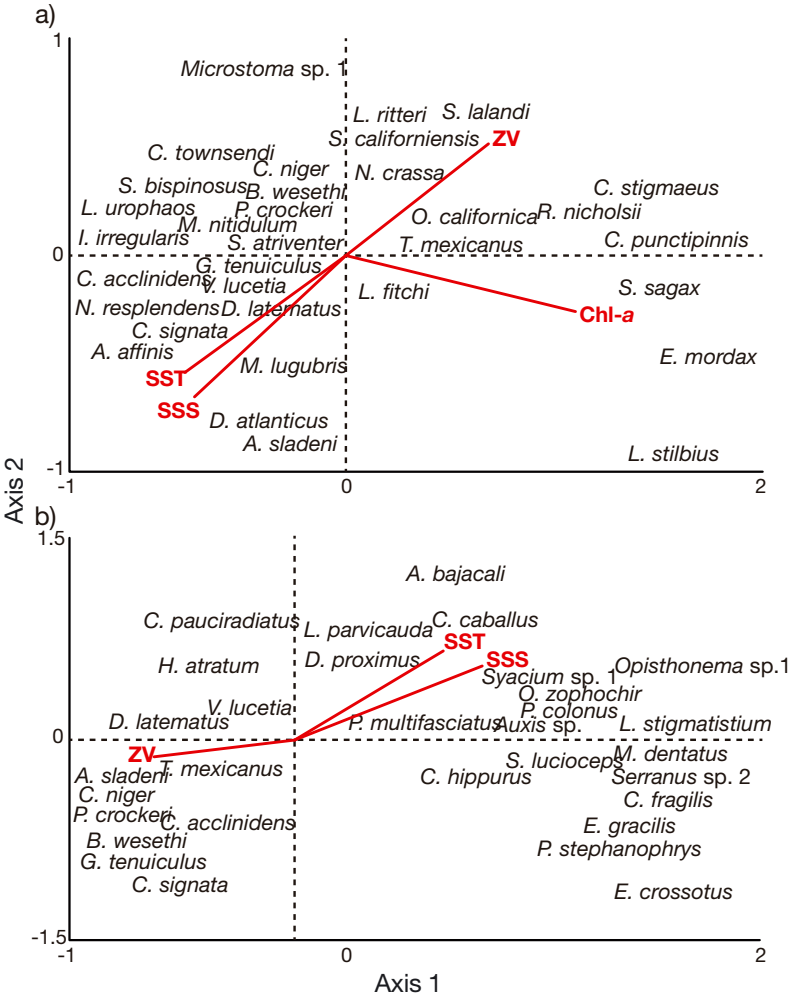

Fig. 8. As in Fig. 7, but for summer 2014 (cruise BIPOCO-1407)

Conditions associated with LN 2011–2012 in the CCS remained among the lowest temperature values for an above-average upwelling event since 1998 from central California to Baja California (Bjorkstedt et al. 2011). These conditions off the WBCP promoted an increase in productivity, as well as slightly above-average chl *a* values during the summer and fall of 2011 (Wells et al. 2013). In the summer of 2014, the influence of tropical and equatorial oligotrophic waters (StSW and ESsW) increased and advanced as far as Bahía Sebastián Vizcaíno, and by 2015, it reached as far as Ensenada. The highest temperature anomalies (+2°C) in the CCS during 2014 occurred due to the intrusion of the MHW (The Blob) off WBCP (Cavole et al. 2016). The sinking of CC water under the warmer surface water (particularly in the southern CCS) led to a deepening of the nutricline, weak upwellings, increased stratification, and decreased phytoplankton biomass (Durazo et al. 2017, Gómez-Ocampo et al. 2018). Environmental condi-

tions between the strong LN 2010–2011 and the warm period of The Blob 2014 and EN 2015 led to a 68% decrease in the average chl *a* concentration we found north of PE. Likewise, the impact on the ZV was a reduction of 42% in the northern and 71% in the southern region.

4.2. Fish larval abundance

The combination of the 2013–2016 warm events such as The Blob and EN (Jacox et al. 2016) created an unprecedented warm period which resulted in a significant decrease in primary and secondary production. In the case of the WBCP, the average ZV values and fish larval abundance decreased drastically in this transition of conditions. The reduction in ZV in the southern region of the CC was accompanied by an important change in species composition. During 2011, gelatinous organisms (jellyfish and salps) were predominant, while crustaceans and other predatory organisms had low abundance (Wells et al. 2013, Lavaniegos et al. 2015). In contrast, in the summer of 2014, the ZV decline coincided with a drastic decrease in gelatinous zooplankton, while copepods and euphausiids accounted for almost 60% of the abundance, followed by chaetognaths (11–19.6%) (Sarmiento-Lezcano 2018).

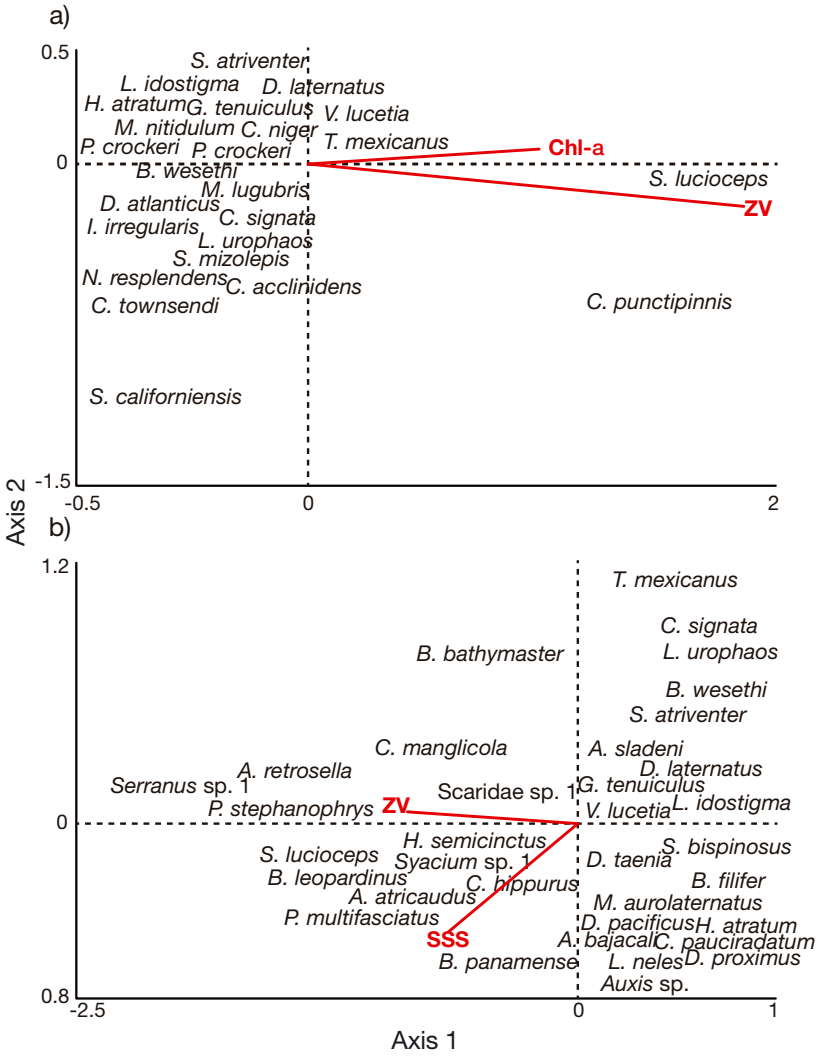

Fig. 9. As in Fig. 7, but for summer–fall 2015 (cruise BIPOCO-1509)

During the 2011–2012 cold period, the high density of herbivorous gelatinous zooplankton seemed to determine the function of the WBCP pelagic ecosystem (Bjorkstedt et al. 2012). Its high abundance is a result of its rapid growth rates, short generation times, and very high filtration rates during greater primary and secondary production periods (Madin et al. 2006) such as LN 2011, which was favorable to the spawning fishes in the region. This high production period may explain the higher abundance of larvae in 2011 in relation to 2014 and 2015.

The changes in fish larval composition and abundance were among the most extreme recorded for the WBCP, but they differed between the northern and southern regions of PE. The larval density between the fall of 2011 and the summer–fall of 2015 decreased by 74% in the northern region, while south of PE, it decreased by 82%. This was consistent with the 80% reduction in the copepod abundance between the summer of 2014 and summer–fall of 2015 (La Rosa-Izquierdo 2018). Additionally, when comparing the northern region winters of 2012 and 2016, the abundance of planktonic mollusks decreased by 26%, which is also consistent (Moreno-Alcántara 2021).

There were clear differences between strong EN event effects in the WBCP. During the EN of 1997–1998, the average larval abundance in summer for the northern region of the WBCP was 666 and 605 organisms per 10 m^2 for 1997 and 1998, respectively (Jiménez-Rosenberg et al. 2007). These values are slightly higher than those in the fall of LN 2011 (515 organisms per 10 m^2), but twice the values observed in the summer of 2014, and furthermore, almost 5 times the values in the summer–fall of 2015 (136 organisms per 10 m^2).

On the other hand, during LN 1999–2000 in the northern region, the larval density recorded in the summer of 1999 was 344 organisms per 10 m^2 (Aceves-Medina et al. 2018), similar to what was observed during the summer of 2014. It is likely that the lower larval fish density in summer LN 1999–2000 in contrast to LN 2010–2011 was due to a delay in the breeding season of temperate-affinity fish, as was suggested in the case of euphausiids, where the strong effects of EN 1997–1998 delayed the increase in abundance of temperate species such as *Euphausia pacifica* and *Thysanoessa spinifera* (Gaxiola-Castro et al. 2008, Parés-Escobar et al. 2018).

Although the comparison of larval abundance and composition was made only with the equivalent stations for the 3 cruises (thus eliminating the difference in the spatial coverage), some of the variability could be due to differences in the seasonality of the cruises. For example, the temporal coincidence of the 2011 and 2015 cruises was in October (early fall) while the overlap of the 2014 and 2015 cruises was in September (late summer). However, according to Jiménez-Rosenberg et al. (2007, 2010, 2020), the main changes in species composition and diversity occur between fall and winter as well as between spring and summer, but the larval fish community is quite similar between summer and fall. The same authors mentioned that the most important change between summer and fall is an increase in the abundance of larvae towards the fall. We describe the opposite effect, i.e. a decrease in abundance from the fall of 2011 to the summer of 2014, and the summer–autumn of 2015, allowing us to assume that the observed effect was not related to seasonal variability, but was due to interannual variability.

The decline in larval fish density has been related to the ocean-to-shore transport of lipid-deficient copepods during The Blob in 2014 along the US coast (Peterson et al. 2017). During this year, these deficiencies spread throughout the food chain, resulting in poor feeding conditions for fish larvae (Leising et al. 2015). The continued presence of oligotrophic waters until 2015, associated with The Blob and EN, influenced the decline in zooplankton abundance, and prolonged the low-abundance period and the food quality for fish larvae. The magnitude of change in fish larval density within the southern (74%) and northern regions (82%) of the WBCP places this period as the most extreme ever recorded. The maximum decline between periods of high and low fish larval abundance between 1951 and 2008 from Central California to Baja California was 63% (Koslow et al. 2019).

4.3. Species composition and larval fish assemblages

A total of 341 taxa of fish larvae were previously recorded from almost 20 yr of sampling (1997–2016) in the northern region of the WBCP (Jiménez-Rosenberg et al. 2020). Notably, 421 taxa were recorded in our study. This can be attributed in part to the greater latitudinal spatial coverage, mainly to the south of the Gulf of Ulloa where IMECOCAL Program cruises have not been conducted. However, it is also likely due to the wide range of environmental conditions between LN 2010–2011 and EN 2015–2016, which brought diverse assemblages with different biogeographic affinities in a relatively short period.

The latitudinal environmental gradients, which according to the analyses denoted 2 distinct ecosystems, determined not only notable differences in the larval abundance as well as in the structure of fish larval assemblages, but also different responses to intra-annual variability and the way in which the community is affected by the environmental variables inside each region north and south of PE. For example, although the dominant species for the 3 surveys were mostly mesopelagic (23 taxa), 3 demersal, and 1 coastal epipelagic, there were 9 mesopelagic species and 2 demersal species exclusive to the northern region, while in the southern region, the exclusive species were mostly demersal and epipelagic (15 species), only 2 of them being mesopelagic.

Studies on the effect of The Blob and EN 2015–2016 demonstrate there was an anomalous invasion of tropical species in the central and northern regions of the CCS (Auth et al. 2015, 2018, Walker et al. 2020, Nielsen et al. 2021). Hence, we expected greater change in the fish larval community north of PE due to the anomalous intrusion of warmer water masses (StSW and Tropical Surface Water, TSW) than in the southern region, where these water masses are common. However, intense and in some cases greater changes were observed in the region south of PE. For example, the number of dominant species remained the same during the 3 cruises in the northern region (4 to 6 species), while in the south, the dominant species increased from 6 to 26. The maximum increase in species richness was in the southern region (44%), consistent with the increase in the number of tropical and subtropical species from 54 to 88.

In the northern region, during 2011, the relative abundance of demersal species (45.3%) was similar to that of mesopelagics (51.8%), but in 2014 and 2015, there was an increase in the number of mesopelagic species, as well as in their relative abundance

(97 and 88%, respectively). The opposite effect occurred in the south, where in 2011, the relative abundance of demersal species (66.1%) was higher than that of mesopelagic species (26.8%), but in 2014 and 2015, despite the increase in the number of demersal species, the relative abundance was practically the same in both groups (47.3 vs. 49.3%). These results demonstrate a latitudinal segregation with opposite effects in the community structure, in which the alternation in the dominance of mesopelagic and demersal species established the main difference between the cold and warm periods. However, this is not a rule, since, for example, during LN 1999–2000, the summer was characterized by extremely low diversity and abundance of demersal species in the north, where only *S. guttata* (temperate affinity) and *P. stephanophrys* (subarctic–subtropical affinity) were found among the 21 dominant species, and their abundance did not reach more than 2.6% of the total (Aceves-Medina et al. 2018), quite similar to the conditions found during the warm events of 2014–2015. Unlike LN 2010–2011, which was preceded by a predominantly cold period, LN 1999–2000 followed the EN 1997–1998, one of the three most intense warm events of the last 5 decades. This condition caused a delay in the increase in the abundance of temperate species such as the euphausiids *E. pacifica* and *T. spinifera* (Gaxiola-Castro et al. 2008, Parés-Escobar et al. 2018) and seems to have determined a delay in the reproductive periods of temperate fish species.

Despite the intensity of the warming episodes that prevailed during 2011–2015, no range expansions in the latitudinal distribution occurred, since all species found in this study were previously recorded in the WBCP (Fischer 1995, Moser & Smith 1993, Froese & Pauly 2019). Coastal demersal species of tropical affinity were present south of PE during the summer of 2014, but they were found as far as Punta Banda (29° N) in 2015. In both cases, the distribution area coincided with the most intense northward geostrophic flow over the coastal area. However, the demersal species that increased their larval abundance in the north (such as *P. stephanophrys*, *S. lucioceps*, or *Etropus crossotus*), plus those that first appeared in this region during 2015 (*Ctenogobius manglicola*, *H. semicinctus*, and *Serranus*) have local adult populations registered north of PE (Fischer 1995, Froese & Pauly 2019).

In contrast, the larvae of demersal species whose adults are distributed exclusively to the south, such as *Paranthias colonus*, *B. bathymaster*, *B. leopardinus*, *Aulopus bajacali*, and *S. ovale* (Fischer 1995, Froese & Pauly 2019), did not cross the transition zone off Bahía Sebastián Vizcaíno. All of these demersal species have their maximum reproduction period in summer and fall, and their abundance increases under warming conditions (Jiménez-Rosenberg et al. 2007, Aceves-Medina et al. 2018). Thus, the increase in the number of tropical demersal species north of PE corresponds to taxa that, although in low abundance, have already been recorded previously as larvae and adults in the study area in normal years. *S. lucioceps*, *P. stephanophrys,* and *O. scrippsae* (demersal–subtropical) belong to the characteristic assemblage of the coastal central region of the WBCP that increases its abundance during cold years (Moser & Smith 1993). This group showed no significant latitudinal changes in its distribution during the 3 years studied, but a decrease in its abundance during the warm period 2014–2015 was observed. These results also demonstrate a low latitudinal dispersion of demersal species despite southward coastal flows during LN and northward during EN.

These findings suggest that the physical barriers established by eddies and environmental gradients off PE were not crossed in summer by most larvae of demersal species with tropical distribution, even in the presence of the intense EN 2015–2016. Mahimahi *C. hippurus* rarely spawns in southern California, but eggs were found there during the summer of 2014 (Leising et al. 2015). However, the northernmost location of *C. hippurus* larvae in this work was off Punta Banda in 2011 and 2015, while it was only observed south of PE in 2014. We did not analyze fish eggs; however, if reproduction occurred in 2014 and 2015 north of PE as reported by Leising et al. (2015) for southern California, larval survival should have been very low.

The ocean shore gradients observed in the abundance of the assemblages at the northern region of the WBCP seem to be associated with the effects of The Blob during 2014. According to Peterson et al. (2017), The Blob began in Oregon and California during the early summer of 2014 and lasted until 2015, causing an increase in the species richness of dinoflagellates and rare copepod oceanic species from warm waters and lipid-poor compositions. This finding supports the hypothesis that water sources came from offshore due to advection associated with The Blob (Leising et al. 2015). In this work, there was an increase in the species richness and abundance in the northern region mainly for mesopelagic species; the offshore influx of oceanic species during 2014 and 2015 was evident by the distribution of fish larval assemblages. The highest larval abundance of mesopelagic species in the wide distribution group (*D. lat-*

ernatus, T. mexicanus, and *B. wesethi*), as well as the northern oceanic groups (NO1 and NO2), were closer to the coast during 2014 than during 2011. Likewise, the distribution of northern groups of demersal and small epipelagic species was closer to the coast in 2014 than in 2011, and some of them were not present during 2015. The influx of warm oceanic water into this area was also suggested by Aceves-Medina et al. (2020) due to the presence of holoplanktonic mollusks with affinity to warm waters of the Central Pacific, such as *Atlanta rosea* and *A. fragilis*.

During 2015, the distribution boundary of the northern oceanic and coastal groups shifted offshore mainly in the south, most likely due to the combined condition of a decrease in the effect of The Blob and the presence of southern waters along the coast, related to EN. The main difference in 2015, in the northern region of the WBCP, was a decrease in the abundance of coastal species of cold affinity, such as *Citharichthys stigmaeus* and *Paralabrax maculatofasciatus*, in group NC1, *C. xanthostigma* in NC2, and *Symphurus atricauda* in NC4. Conversely, an increase in warm-water-related flounders was observed off Oregon and California (Leising et al. 2015).

Despite representing a large marine ecosystem with distinctive characteristics (Sherman & Duda 1999), the CCS is susceptible to different regional oceanographic processes that affect each region differently (Koslow et al. 2019). In the case of fish, the region between Pt. Concepcion, USA, and Ensenada, Mexico, constitutes an ecotone between cold- and warm-water fauna, with divergent responses in species of mesopelagic fishes, to cyclical processes such as ENSO and PDO (Koslow et al. 2019). This seems to be the case in the transition zone in the mid-peninsula area between Punta Baja and PE, where mesoscale oceanographic processes, such as the semi-permanent system of cyclonic and anticyclonic eddies, establish barriers between the communities of southern and northern faunas in groups such as copepods (La Rosa-Izquierdo 2018), atlantid heteropods (Aceves-Medina et al. 2020), and fish larvae (Aceves-Medina et al. 2019). Due to the strong latitudinal environmental gradient between both sides of the peninsula, the explained variance in the PCA was higher than 60% on the first 2 axes and was mainly determined by SST and SSS, which explain the separation between a northern community of temperate affinity and a tropical southern one. Within each region (northern and southern), the latitudinal gradients of the physical variables decreased considerably, so that the variance explained in the CCA was lower than 34% in all cases; however, this allowed us to detect a division between demersal and mesopelagic communities, associated with the effect of the coast–ocean gradients of chl *a* and ZV.

In the northern region of the WBCP, the CCA dispersion diagram showed that the variables determining the species abundance patterns were mainly related to the ocean–coastal gradients of chl *a* and ZV, with opposite effects on the distribution of the oceanic mesopelagic species and the neritic community of epipelagic and demersal species. The narrow continental shelf and the intense upwelling zone located between Ensenada and Punta Baja (Durazo 2015), determined a stronger ocean–coastal gradient of chl *a* and ZV than in the south. In addition, the increase in primary production induced by the effects of LN 2011 (Bjorkstedt et al. 2011) seems to have determined the growth of zooplankton and favored the spawning of epipelagic and demersal species, which were co-dominant in abundance with mesopelagic species.

Mesopelagic species mainly feed on zooplankton, but they may have herbivorous habits during periods of low food availability (Catul et al. 2011). Because of this opportunistic behavior, interannual variability seems to act more on species abundance than on species composition (McClatchie et al. 2018). Thus, during the warm period of 2014–2015, the ocean–coast gradient persisted as observed in the CCA, but with a clear decrease in chl *a* and ZV values, as well as a strong change in species composition, where mesopelagics were the dominant component of the community. Only in 2014, the SST and SSS showed mainly an ocean–coastal gradient that correlated with axis 1 in the CCA. This was probably associated with The Blob, where warm oligotrophic water from the central Pacific penetrated into the northern region, favoring the approach to the coast of the mesopelagic fish assemblages.

Off Bahía Sebastián Vizcaíno and the southern region of the WBCP, the wider continental shelf allows a suitable habitat for the reproduction of demersal species. The ocean–coast gradient was maintained, determining the separation of an oceanic environment of low ZV and dominance of mesopelagic species, from a neritic environment of higher ZV concentration and demersal and epipelagic species. In the south, chl *a* was not important for the distribution of species, and SSS was relevant only in 2014. These last 2 results are due to the extremely low chl *a* values during 2014 and 2015 and the warm water input along the coast during 2014.

These characteristics drive different responses to EN, LN, and the MHW events that should be consid-

ered to determine the general change patterns pertaining to these events in the CCS. In addition, the extreme values of decreasing larval density as well as the changing composition and distribution of fish larval assemblages, establish reference patterns for studies about pelagic ecosystem resilience in the southern region of the CC.

Data availability. The data that support the findings of this study are available from the corresponding author upon reasonable request.

Acknowledgements. We thank the Instituto Politécnico Nacional and Secretaría de Investigación y Posgrado project SIP: 20200686, EDI, COFAA, and SNI Grants. We also thank the Instituto Nacional de Pesca for the use of the RV 'BIPO-INAPESCA'.

LITERATURE CITED

Aceves-Medina G, Jiménez-Rosenberg SPA, Saldierna-Martínez RJ, Durazo R and others (2018) Distribution and abundance of the ichthyoplankton assemblages and its relationships with the geostrophic flow along the southern region of the California Current. Lat Am J Aquat Res 46:104–119

Aceves-Medina G, Jiménez-Rosenberg SPA, Durazo R (2019) Fish larvae as indicator species of interannual environmental variability in a subtropical transition area off the Baja California peninsula. Deep Sea Res II 169-170:104631

Aceves-Medina G, Moreno-Alcántara M, Durazo R, Delgado-Hofmann D (2020) Distribution of Atlantidae species (Gastropoda: Pterotracheoidea) during an El Niño event in the Southern California Current System (summer–fall 2015). Mar Ecol Prog Ser 648:153–168

Auth TD, Brodeur RD, Peterson JO (2015) Anomalous ichthyoplankton distributions and concentrations in the northern California Current during the 2010 El Niño and La Niña events. Prog Oceanogr 137:103–120

Auth TD, Daly EA, Brodeur RD, Fisher JL (2018) Phenological and distributional shifts in ichthyoplankton associated with recent warming in the northeast Pacific Ocean. Glob Change Biol 24:259–272

Beers JR (1976) Determination of zooplankton biomass. In: Steedman HF (ed) Zooplankton fixation and preservation. Monographs on Oceanographic Methodology No. 4. UNESCO Press, Paris, p 35–74

Bjorkstedt EP, Goericke R, McClatchie S, Weber E and others (2011) State of the California Current 2010–2011: regionally variable responses to a strong (but fleeting?) La Niña. Calif Coop Ocean Fish Invest Rep 52:36–68

Bjorkstedt EP, Goericke R, McClatchie S, Weber E and others (2012) State of the California Current 2011–2012: Ecosystems respond to local forcing as La Nina wavers and wanes. Calif Coop Ocean Fish Invest Rep 53:41–76

Catul V, Gauns M, Karuppasamy PK (2011) A review on mesopelagic fishes belonging to family Myctophidae. Rev Fish Biol Fish 21:339–354

Cavole LM, Demko AM, Diner RE, Giddings A and others (2016) Biological impacts of the 2013–2015 warm-water anomaly in the Northeast Pacific: winners, losers, and the future. Oceanography 29:273–285

Durazo R (2015) Seasonality of the transitional region of the California Current System off Baja California. J Geophys Res Oceans 120:1173–1196

Durazo R, Baumgartner T (2002) Evolution of oceanographic conditions off Baja California: 1997–1999. Prog Oceanogr 54:7–31

Durazo R, Ramírez-Manguilar AM, Miranda LE, Soto-Mardones LA (2010) Climatología de variables ambientales. In: Gaxiola-Castro G, Durazo R (eds) Dinámica del ecosistema pelágico frente a Baja California 1997–2007. SEMARNAT, INE, CICESE & UABC, Mexico City, p 25–58

Durazo R, Castro R, Miranda LE, Delgadillo-Hinojosa F, Mejía-Trejo A (2017) Anomalous hydrographic conditions off the northwestern coast of the Baja California Peninsula during 2013–2016. Cienc Mar 43:81–92

Eschmeyer WN, Fricker R, Van der Laan R (2019) Eschmeyer's catalog of fishes: genera, species, references. http://researcharchive.calacademy.org/research/ichthyology/catalog/fishcatmain.asp (accessed 19 July 2023)

Fiedler PC, Mantua NJ (2017) How are warm and cool years in the California Current related to ENSO? J Geophys Res Oceans 122:5936–5951

Fischer W (1995) Guía FAO para la identificación de especies para los fines de la pesca. Pacífico centro-oriental. Vertebrados, Vol II & III. FAO, Rome

Froese F, Pauly D (2019) FishBase. www.fishbase.org (accessed 23 Jun 2019)

Gaxiola-Castro G, Durazo R, Lavaniegos B, De La Cruz-Orozco ME, Millán-Núñez E, Soto-Mardones L, Cepeda-Morales J (2008) Pelagic ecosystem response to interannual variability off Baja California. Cienc Mar 34: 263–270

Gómez-Ocampo E, Gaxiola-Castro G, Durazo R, Beier E (2018) Effects of the 2013–2016 warm anomalies on the California Current phytoplankton. Deep Sea Res II 151: 64–76

Jacox MG, Hazen EL, Zaba KD, Rudnick DL, Edwards CA, Moore AM, Bograd SJ (2016) Impacts of the 2015–2016 El Niño on the California Current System: early assessment and comparison to past events. Geophys Res Lett 43:7072–7080

Jacox MG, Alexander MA, Mantua NJ, Scott JD, Hervieux G, Webb RS, Werner FE (2018) Forcing of multiyear extreme ocean temperatures that impacted California Current living marine resources in 2016. Bull Am Meteorol Soc 99:S27–S33

Jiménez-Rosenberg SPA, Saldierna-Martínez RJ, Aceves-Medina G, Cota-Gómez VM (2007) Fish larvae in Bahía Sebastián Vizcaíno and the adjacent oceanic region, Baja California, México. Check List 3:204–223

Jiménez-Rosenberg SPA, Saldierna-Martínez RJ, Aceves-Medina G, Hinojosa-Medina A, Funes-Rodríguez R, Hernández-Rivas M, Avendaño-Ibarra R (2010) Fish larvae off the northwestern coast of the Baja California Peninsula, Mexico. Check List 6:334–349

Jiménez-Rosenberg SPA, Saldierna-Martínez R, Aceves-Medina G (2020) Updated taxonomic list of fish larvae from Bahía Sebastián Vizcaíno, Baja California, México. CICIMAR Oceánides 35:55–70

Koslow JA, Davison P, Ferrer E, Jiménez Rosenberg SPA, Aceves-Medina G (2019) The evolving response of mesopelagic fishes to declining midwater oxygen concentrations in the southern and central California Cur-

rent. ICES J Mar Sci 76:626–638
La Rosa-Izquierdo IY (2018) Estructura de la comunidad de copépodos pelágicos en la costa oeste de la península de Baja California, antes y durante El Niño 2015. MSc dissertation. Instituto Politécnico Nacional, La Paz
Lavaniegos BE, Molina-González O, Murcia-Riaño M (2015) Zooplankton functional groups from the California Current and climate variability during 1997–2013. CICIMAR Oceánides 30:45–62
Leising AW, Schroeder ID, Bograd SJ, Abell J, Durazo R, Gaxiola-Castro G, Warybok P (2015) State of the California Current 2014–15: impacts of the warm-water 'Blob'. Calif Coop Ocean Fish Invest Rep 56:31–68
Madin LP, Kremer P, Wiebe PH, Purcell JE, Horgan EH (2006) Periodic swarms of the salp *Salpa aspera* in the Slope Water off the NE United States: biovolume, vertical migration, grazing, and vertical flux. Deep Sea Res I 53:804–819
McClatchie S, Gao J, Drenkard EJ, Thompson AR and others (2018) Inter-annual and secular variability of larvae of mesopelagic and forage fishes in the southern California Current System. J Geophys Res Oceans 123:6277–6295
McCune B, Grace JB (2002) Analysis of ecological communities. MJM, Gleneden Beach, OR
Moreno Alcántara M (2021) Variación intra e interanual de Atlantidae (Pterotracheoidea) en la costa del Pacífico de Baja California. PhD dissertation, Instituto Politécnico Nacional, La Paz
Moser HG (1996) The early stages of fishes in the California Current region. CalCOFI Atlas No. 33. Allen Press, Lawrence, KS
Moser HG, Smith PE (1993) Larval fish assemblages in the California Current region and their horizontal and vertical distributions across a front. Bull Mar Sci 53: 645–691
Nielsen JM, Rogers LA, Brodeur RD, Thompson AR and others (2021) Responses of ichthyoplankton assemblages to the recent marine heatwave and previous climate fluctuations in several Northeast Pacific marine ecosystems. Glob Change Biol 27:506–520
Parés-Escobar F, Lavaniegos BE, Ambriz-Arreola I (2018) Interannual summer variability in oceanic euphausiid communities off the Baja California western coast during 1998–2008. Prog Oceanogr 160:53–67
Peterson WT, Fisher JL, Strub PT, Du X, Risien C, Peterson J, Shaw CT (2017) The pelagic ecosystem in the Northern California Current off Oregon during the 2014–2016 warm anomalies within the context of the past 20 years. J Geophys Res Oceans 122:7267–7290
Rudnick DL, Zaba KD, Todd RE, Davis RE (2017) A climatology of the California Current System from a network of underwater gliders. Prog Oceanogr 154:64–106
Sarmiento-Lezcano AM (2018) Dinámica de la capa de dispersión profunda en el Pacífico noroeste de México. MSc dissertation. Instituto Politécnico Nacional, La Paz
Sherman K, Duda AM (1999) Large marine ecosystems: an emerging paradigm for fishery sustainability. Fisheries 24:15–26
Smith PE, Richardson SL (1977) Standard techniques for pelagic fish egg and larval surveys. Fish Tech Pap 175. FAO, Rome
Thompson AR, Ben-Aderet NJ, Bowlin NM, Kacev D, Swalethorp R, Watson W (2022) Putting the Pacific marine heatwave into perspective: the response of larval fish off southern California to unprecedented warming in 2014–2016 relative to the previous 65 years. Glob Change Biol 28:1766–1785
Valle-Rodríguez J, Trasviña-Castro A (2017) Poleward currents from coastal altimetry: the west coast of Southern Baja California, Mexico. Adv Space Res 59:2313–2324
Walker HJ Jr, Hastings PA, Hyde JR, Lea RN, Snodgrass OE, Bellquist LF (2020) Unusual occurrences of fishes in the Southern California Current System during the warm water period of 2014–2018. Estuar Coast Shelf Sci 236
Wells BK, Schroeder ID, Santora JA, Hazen EL and others (2013) State of the California Current 2012–13: no such thing as an 'average' year. Calif Coop Ocean Fish Invest Rep 54:37–71
Zaitsev O, Trasviña-Castro A, Linero-Cueto J, Gaxiola-Castro G, Cepeda-Morales J (2014) Oceanographic conditions over the continental shelf off Magdalena Bay (Mexico) in 2011–2012. Cienc Mar 40:89–112

Editorial responsibility: Andrea Anton (Guest Editor), Esporles, Spain
Reviewed by: P. Pepin and 1 anonymous referee

Submitted: August 12, 2022
Accepted: May 16, 2023
Proofs received from author(s): July 22, 2023